

[Supplementary information file]

Continuous selective deoxygenation of palm oil for renewable diesel production over Ni catalysts supported on Al₂O₃ and La₂O₃-Al₂O₃

Kyriakos N. Papageridis,^a Nikolaos D. Charisiou,^a Savvas Douvartzides,^{a,b} Victor Sebastian,^{c,d,e} Steven J. Hinder,^f Mark A. Baker,^f Sara I. AlKhoori,^g Kyriaki Polychronopoulou,^{g,h} and Maria A. Goula^{*,a}

^a Laboratory of Alternative Fuels and Environmental Catalysis (LAFEC), Department of Chemical Engineering, University of Western Macedonia, GR-50100, Greece; Tel: +30 24610 68296; E-mail: mgoula@uowm.gr

^b Department of Mechanical Engineering, University of Western Macedonia, GR-50100, Greece

^c Department of Chemical Engineering and Environmental Technology, Universidad de Zaragoza, Campus Río Ebro-Edificio I+D, 50018 Zaragoza, Spain

^d Instituto de Nanociencia y Materiales de Aragón (INMA), Universidad de Zaragoza- CSIC, c/ María de Luna 3, 50018 Zaragoza, Spain

^e Networking Research Center on Bioengineering, Biomaterials and Nanomedicine, CIBERBBN, 28029 Madrid, Spain

^f The Surface Analysis Laboratory, Faculty of Engineering and Physical Sciences, University of Surrey, Guildford, GU2 4DL, UK

^g Department of Mechanical Engineering, Khalifa University of Science and Technology, Abu Dhabi, P.O. Box 127788, UAE

^h Center for Catalysis and Separations, Khalifa University of Science and Technology, Abu Dhabi, P.O. Box 127788, UAE

*Corresponding author: Prof. Maria A. Goula
Postal Address: University of Western Macedonia
Department of Chemical Engineering
Laboratory of Alternative Fuels and Environmental Catalysis
Koila, Kozani, 50100, Greece
e-mail: mgoula@teiwu.gr
Telephone: +30 24610 68296

RESULTS & DISCUSSION

Catalysts characterization

Inductively Coupled Plasma Atomic Emission Spectroscopy

Elemental analysis (ICP-AES), carried out on the calcined catalysts showed that the desired Ni loading was achieved for both as it was found equal to 7.83 wt.% for the Ni/Al and 7.92 wt.% for the Ni/LaAl. Moreover, ICP measurements on the spent catalysts obtained after the long time-on-stream tests (experimental protocol #2) showed no significant difference between calcined and spent samples as the Ni loading recorded for the latter catalysts was found to be equal to 7.80 wt.% (Ni/Al) and 7.90 wt.% (Ni/LaAl). It is noted that the methodology followed and instrument used has been described in detail previously [1].

N₂ Adsorption-Desorption Isotherms and Pore Size Distribution

Figure S1a,b presents the N₂ adsorption-desorption isotherms obtained for the calcined Ni/Al and Ni/LaAl catalysts. According to the International Union of Pure and Applied Chemistry (IUPAC) classification, the Ni/Al catalyst presents a type IV isotherm with an H2 hysteresis loop, which indicates the presence of non uniform size or shape. However, the Ni/LaAl catalyst presents a type III isotherm with an H3 hysteresis loop, which indicates the presence of particles agglomerates forming non uniform slit shaped pores [2,3]. The BJH adsorption data (insets in Figure S1a,b), for both catalytic materials, show that the majority of the population of pores is in the meso-range and has a bimodal distribution in the range of 10-75 nm.

X-ray Diffraction Analysis

Figure S1c presents the X-ray diffractograms of the calcined Ni/Al and Ni/LaAl catalysts. For both materials, characteristic peaks assigned to γ -Al₂O₃ ($2\theta = 35.2^\circ, 47.2^\circ$ and 67.6°) and the spinel nickel aluminate phase (NiAl₂O₄, $2\theta = 19.0^\circ, 32.0^\circ, 37.0^\circ, 45.0^\circ, 60.2^\circ$ and 65.9°) can be observed. However, no peaks corresponding to the nickel oxide (NiO) structure were detected, which indicates that these crystalline phases would be quite small and well dispersed [4]. It is noteworthy that the peaks corresponding to the spinel phase are somehow suppressed, in the case of the Ni/LaAl catalyst, suggesting that a finer dispersion was achieved as a result of the competitive growth of the La₂O₃ and NiAl₂O₄, where the one phase hinders the growth of the other [5]. Moreover, for the Ni/LaAl catalyst, no diffraction peaks corresponding to the La₂O₃ phase were detected, indicating that either the structure is amorphous or that the La₂O₃ was highly dispersed in the support [6,7].

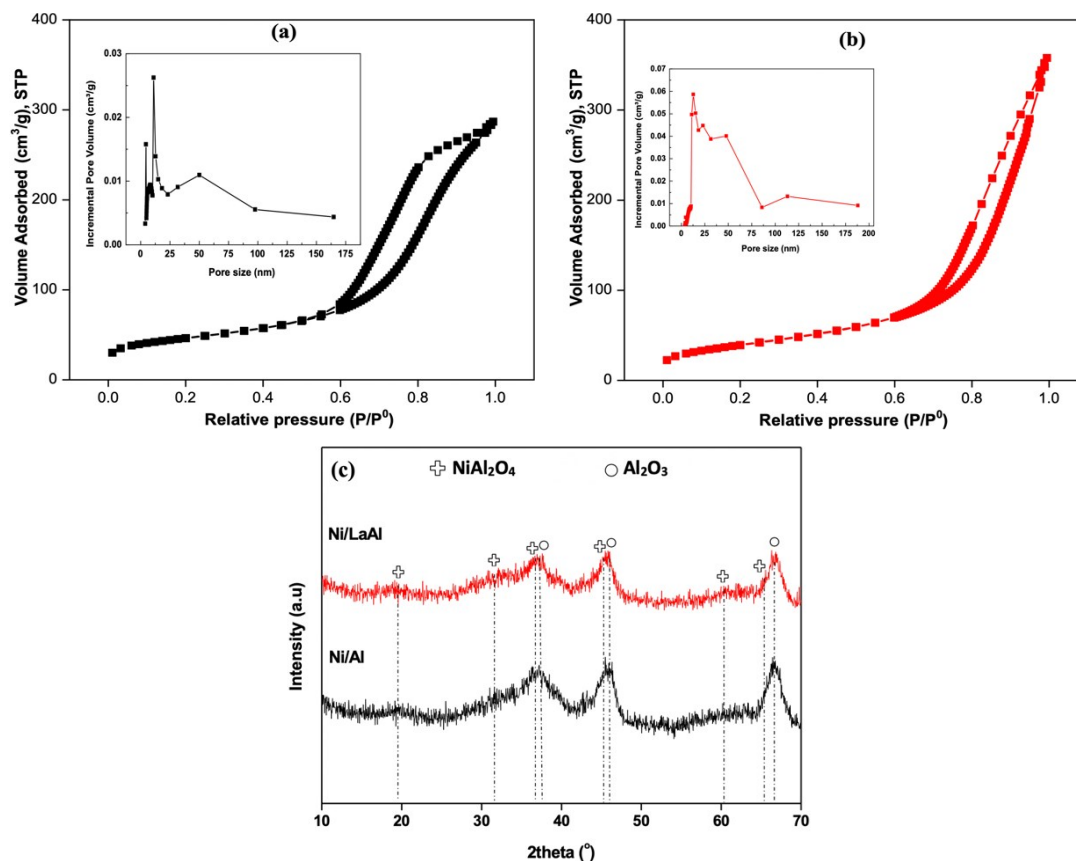


Fig. S1 (a) N₂ adsorption-desorption isotherms and pore size distribution (inset) of the Ni/Al catalyst, (b) N₂ adsorption-desorption isotherms and pore size distribution (inset) of the Ni/LaAl catalyst, and (c) XRD patterns of the Ni/Al and Ni/LaAl catalysts.

H₂ Temperature Programmed Desorption

The results from H₂-TPD experiments are depicted in Figure S2. It is observed that the Ni/Al catalyst shows H₂ desorption peaks at 70, 490 and 720°C, while the Ni/LaAl catalyst at 40, 160, 480, 750 and 810°C. In regards to the mean Ni particle size, it is obvious that the results obtained differ from those obtained via electron microscopy however this discrepancy can be explained on the basis of the techniques used. As an example, it is well known that particle shape has an important effect in the investigation of its chemical/physical properties [8,9], but the chemisorption technique is linked with spherical shapes, which have the lowest surface area per volume ratio of all the geometric shapes [10]. It is noted however that the potential error in the calculation of the particle size by chemisorption does not affect the adsorption strength of the probe molecules (such as hydrogen) to the different exposed facets [11]. The adsorption conditions of probe molecules are also important and one may find reports in the literature demonstrating the need of even cryogenic conditions, to achieve saturation of the metal surfaces with the probe molecule, for a variety of geometries, shapes and sizes [12].

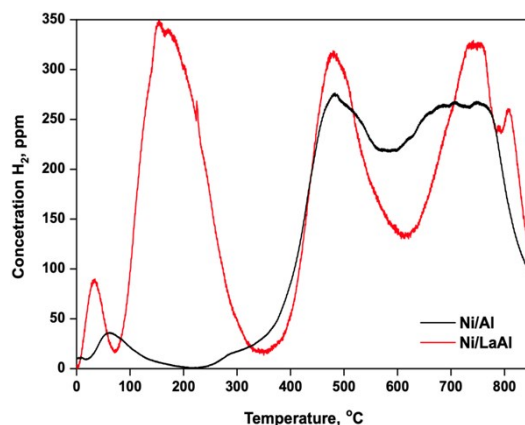


Fig. S2 H₂-TPD profiles obtained over the Ni/Al and Ni/LaAl catalysts.

X-ray Photoelectron Spectroscopy

The high resolution XPS Ni 2p spectra for the reduced Ni/Al and Ni/LaAl catalysts are presented in Figure S3. Firstly, it is noted that the catalysts have been exposed to atmospheric conditions prior to XPS analysis. Secondly, some uncertainty arises in regards to the Ni/LaAl catalyst, as the Ni 2p_{3/2} and La 3d_{3/2} peaks overlap. Nevertheless, through peak fitting the Ni 2p and La 3d peaks and satellites, based upon experimentally determined peak positions and degeneracy ratios for the respective metal oxides/hydroxides [13,14], approximate elemental compositions are given in Table 3. Lastly, small concentrations of carbon (< 5 at.%) were observed on all surfaces and to provide comparative values, the elemental concentrations shown in Table 3 have been normalized after removal of the carbon contribution.

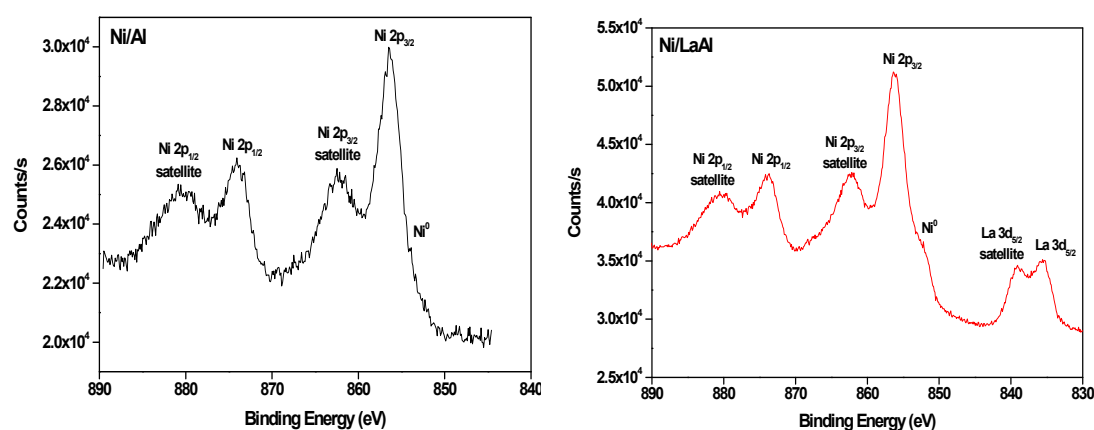


Fig. S3 XPS Ni 2p for the reduced Ni/Al and Ni/LaAl catalysts.

Catalytic activity

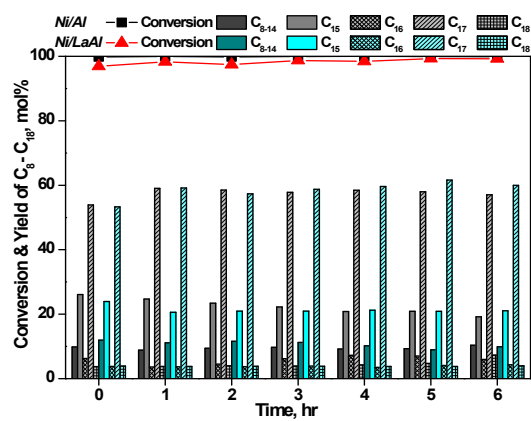


Fig. S4 Palm oil conversion and paraffin yield for the Ni/Al and Ni/LaAl catalysts during 6 h time-on-stream experiments (experimental protocol #1). *Reaction conditions: $T = 375^{\circ}\text{C}$, $P = 30 \text{ bar}$, $LHSV = 1.2 \text{ h}^{-1}$, $H_2/\text{oil} = 1000 \text{ cm}^3/\text{cm}^3$.*

Table S1 Liquid product analysis of non-catalytic experiment (blank experiment). *Reaction conditions: $T = 375^{\circ}\text{C}$, $P = 30\text{ bar}$, $LHSV = 1.2\text{ h}^{-1}$, $H_2/\text{oil} = 1000\text{ cm}^3/\text{cm}^3$.*

Compound (wt.%)	0 h	1 h	2 h	3 h	4 h	5 h	6 h
Total Hydrocarbons	23.35	23.18	22.92	23.05	23.06	22.98	22.97
Octane ($n\text{-C}_8$)	1.82	1.86	1.82	1.83	1.85	1.94	1.89
Nonane ($n\text{-C}_9$)	1.17	1.15	1.09	1.06	1.11	1.15	1.18
Decane ($n\text{-C}_{10}$)	4.74	4.92	4.89	4.95	5.04	4.94	4.89
Undecane ($n\text{-C}_{11}$)	9.60	9.46	9.28	9.31	9.37	9.40	9.50
Pentadecane ($n\text{-C}_{15}$)	2.19	2.17	2.16	2.20	2.13	2.07	2.13
Heptadecane ($n\text{-C}_{17}$)	3.83	3.62	3.68	3.70	3.56	3.48	3.38
Total Fatty Acids	76.65	76.82	77.08	76.95	76.94	77.02	77.03
Stearic Acid ($\text{C}_{18:0}$)	69.42	71.83	70.76	72.18	72.97	73.18	72.85
Oleic Acid ($\text{C}_{18:1}$)	2.41	0.84	1.86	0.84	3.62	3.84	4.18
Palmitic Acid ($\text{C}_{16:0}$)	4.82	4.15	4.46	3.93	0.35	0.00	0.00

Repeatability of experimental work

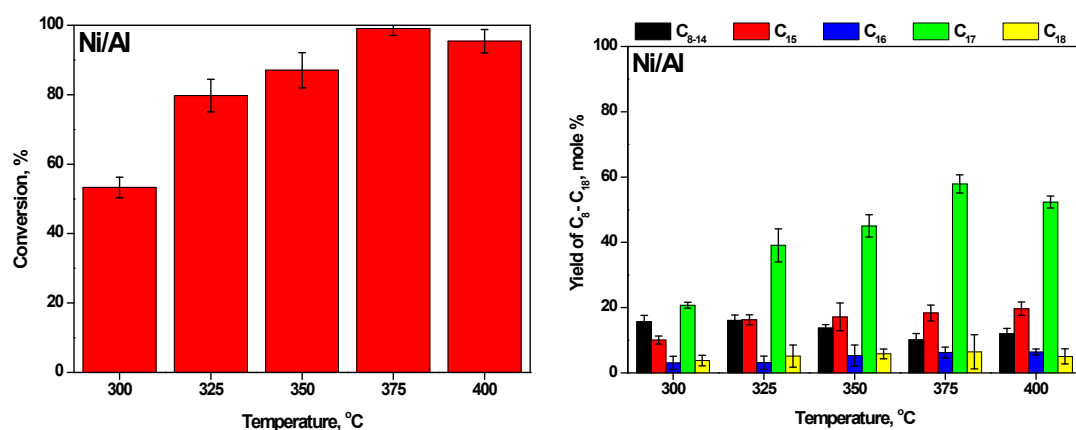


Fig. S5 Repeat experiments for the Ni/Al catalyst tested herein; (left hand side) Conversion (right hand side) Yield of C₈-C₁₈ paraffins (black color: C₈-C₁₄; red: C₁₅; blue: C₁₆, green: C₁₇, yellow: C₁₈).

References

1. M.A. Goula, N.D. Charisiou, K.N. Papageridis, A. Delimitis, E. Pachatouridou, E.F. Iliopoulou, *International Journal of Hydrogen Energy*, 2015, **40**, 9183–9200.
2. K. S. Sing, *Pure and Applied Chemistry*, 1982, **54**, 2201–2218.
3. G. Leofanti, M. Padovan, G. Tozzola and B. Venturelli, *Catalysis Today*, 1998, **41**, 207–219.
4. N. D. Charisiou, V. Sebastian, S. J. Hinder, M. A. Baker, K. Polychronopoulou and M. A. Goula, *Catalysts*, 2019, **9**, 650.
5. H. M. Abdeldayem, M. Faiz, H. S. Abdel-Samad and S. A. Hassan, *Journal of Rare Earths*, 2015, **33**, 611–618.
6. G. Garbarino, C. Wang, I. Valsamakis, S. Chitsazan, P. Riani, E. Finocchio, M. Flytzani-Stephanopoulos and G. Busca, *Applied Catalysis B: Environmental*, 2015, **174-175**, 21–34.
7. C. Melchor-Hernández, A. Gómez-Cortés and G. Díaz, *Fuel*, 2013, **107**, 828–835.
8. Z. Y. Li, N. P. Young, M. Di Vece, S. Palomba, R. E. Palmer, A. L. Bleloch, B. C. Curley, R. L. Johnston, J. Jiang and J. Yuan, *Nature*, 2008, **451**, 46–48.
9. L. M. Molina, S. Lee, K. Sell, G. Barcaro, A. Fortunelli, B. Lee, S. Seifert, R. E. Winans, J. W. Elam, M. J. Pellin, I. Barke, V. Von Oeynhausen, Y. Lei, R. J. Meyer, J. A. Alonso, A. Fraile Rodríguez, A. Kleibert, S. Giorgio, C. R. Henry, K. H. Meiwes-Broer and S. Vajda, *Catalysis Today*, 2011, **160**, 116–130.
10. L. Torrente-Murciano, *Journal of Nanoparticle Research*, 2016, **18**, 87.
11. I. V. Yudanov, R. Sahnoun, K. M. Neyman, N. Rösch, J. Hoffmann, S. Schauer mann, V. Johánek, H. Unterhalt, G. Rupprechter, J. Libuda and H. J. Freund, *Journal of Physical Chemistry B*, 2003, **107**, 255–264.
12. C. Guzmán, G. Del Angel, R. Gómez, F. Galindo, R. Zanella, G. Torres, C. Angeles-Chavez and J. L. Fierro, *Journal of Nano Research*, 2009, **5**, 13–23.
13. A. P. Grosvenor, M. C. Biesinger, R. S. C. Smart and N. S. McIntyre, *Surface Science*, 2006, **600**, 1771–1779.
14. M. F. Sunding, K. Hadidi, S. Diplas, O. M. Løvvik, T. E. Norby and A. E. Gunnæs, *Journal of Electron Spectroscopy and Related Phenomena*, 2011, **184**, 399–409.